Chapter II

Theoretical Backgrounds and literature review

2.1 Photocatalysis process

Photocatalysis process is one of method, which has been applied successfully to purify water and air. This process can be carried out in various media: gas phase, pure organic liquid phases or aqueous solutions (Herrmann, 1999).

Semiconductors (such as TiO_2, ZnO, ZrO_2, CeO_2, CdS, ZnS, etc.) are usually selected as photocatalysts, because semiconductors have a narrow gap between the valence and conduction bands, where as metals have no gap and insulator have a wide gap. TiO_2 has been widely used as a photocatalyst due to its photo-activity, low cost commercial availability, conservative nature, non-toxicity and high stability of light illumination (Oppenlander, 2003).

In order for photocatalysis process to proceed, the semiconductors (SC) need to absorb photon energy equal to or greater than its band-gap energy E_G ($h\nu \geq E_G$). The electron at the valence band will be excited up to the conduction band, with the positive hole being left at the site where the electron is originally captured. These electron-hole pairs can initiate redox reactions leading to a decomposition of pollutants. By the electron can reduce acceptor molecules whereas the positive hole can oxidize donor molecules as shown in equation (1-3).

$$h\nu + (SC) \longrightarrow e^- + p^+ \qquad (1)$$

$$A(ads) + e^- \longrightarrow A^-(ads) \qquad (2)$$

$$D(ads) + p^+ \longrightarrow D^+(ads) \qquad (3)$$

where A is acceptor molecules and D is donor molecules.

Figure 2.1 Scheme of the photocatalytic process
(http://dev.nsta.org/evwebs/1952/photocatalysis.htm)
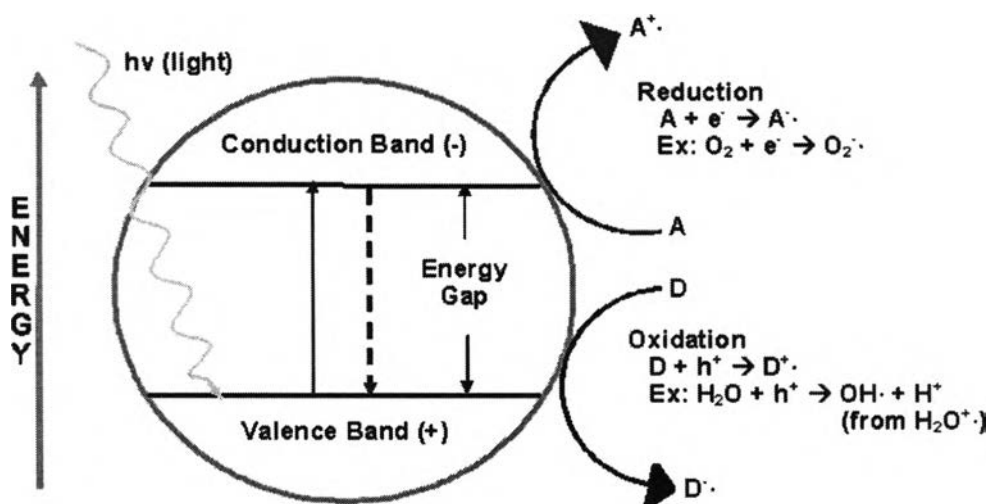
The photo-efficiency can be reduced by the electron-hole recombination, which corresponds to the degradation of the photoelectric energy into heat.

The electron-hole recombination has the resulting effect of reducing the process quantum efficiency. The recombination can occur either between the energy bands (volume recombination) or on the semiconductor surface (surface recombination) as show in figure 2.2.

$$e^- + p^+ \longrightarrow N + E \tag{4}$$

where N is the neutral center and E the energy released under the form of light ($hv' \leq hv$) or of heat.
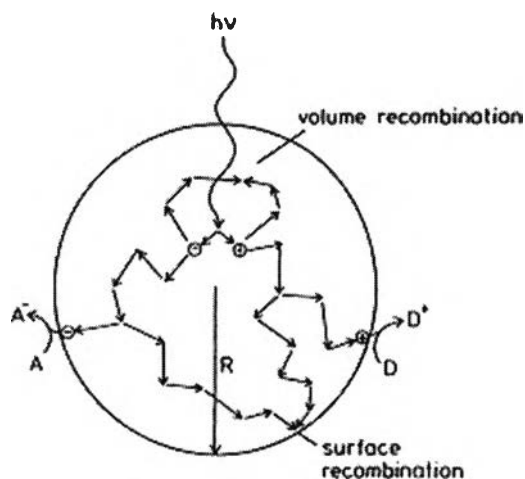
Figure 2.2 Fate of electrons and holes within a spherical particle of catalyst in the

presence of acceptor (A) and donor (D) molecules (Herrmann, 1999)

2.1.1 Advantages of photocatalysis process (Herrmann, 1999)

Advantages of photocatalysis process over other treatment method are as follow:

- cheap chemicals in use

- no additives required (only oxygen from the air)

- system applicable at low concentrations

- great deposition capacity for noble metal recovery

- absence of inhibition or low inhibition by ions generally present in water

- total mineralization achieved for many organic pollutants

- efficiency of photocatalysis with halogenated compounds sometimes very toxic for bacteria in biological water treatment

- possible combination with other decontamination methods (in particular biological)

2.1.2 Concept of photocatalysis process (Kanki et al., 2004).

When semiconductor is illuminated with photons whose energy is equal to or greater than their band-gap energy E_G ($h\nu \geq E_G$), there is absorption of these photons, the electron at the valence band is excited up to the conduction band, with the positive hole being left at the site where the electron is originally captured. The band gap energy of TiO_2 is 3.2 eV, with the lower level being −0.4 eV and the upper level being 2.8 eV relative to the reduction potential of hydrogen. The reduction potential of water lies between the lower and upper levels. The water, thus, can be photochemically decomposed by TiO_2 catalyst. Suppose the water which does contains metallic ions but does not contain dissolved oxygen, it is expected that the excited electron should reduce the metallic ion whereas the positive hole should oxidize the hydroxide ion to produce the hydroxyl radical. And if some organic carbon exists in the water, the hydroxyl radical should oxide it into carbon dioxide and water, thus be consumed by the oxidation process, which results in suppressing the recombination of excited electron with the positive hole. The reduction reaction of metallic ion would then continuously proceed. We here refer such organic carbon to as "hole scavenger" (to inhibit recombination). In this experiment, we selected chromium (VI) for target metal, whose reduction potential is 1.33 eV and lies between the lower and higher levels of the band gap.

2.1.2.1 Concept of photocatalytic-reduction

The photocatalytic-reducition consider from reduction potential of polutant. The photo-reduction will occur when reduction potential of polutant more than reduction potential of e^- conduction band as shown in Figure 2.3. From this figure, it found that the metalic pair PbO_2/Pb^{2+} to Ni^{2+}/Ni^0 can occur the photo-reduction with TiO_2. As the metalic pair Cd^{2+}/Cd^0 to Mn^{2+}/Mn^0 not can occur the photo-reduction with TiO_2.
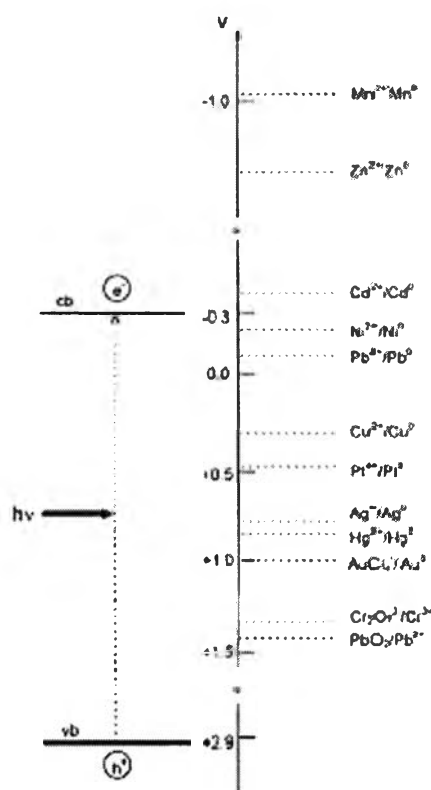
Figure 2.3 Positions of the redox potentials of various metallic couples related to the
energy levels of the conduction and valence bands of TiO_2 Degussa P-25 at
pH 0 (Litter, 1999)

In this experiment, Chromium (VI) was used for target metal, whose reduction
potential is 1.33 eV that can occur the photo-redution.

2.1.3 Application of photocatalysis process:

Matthews (1987) fixed TiO_2 to a stationary support so as to avoid filtration
and resuspension in a water purification process. In this work, 400 mg of TiO_2 was
suspended in 80 cm^3 of water and then sucked into a borosilicate spiral glass tube.
The end of the spiral was closed and vacuum applied while warm air was blown
around the spiral. This process was repeated to build up a successive layer of TiO_2 on
the inside surface of the tube. The effect of the amount of TiO_2 on the tube surface

was studied by application of 50 μM of 500 cm^3 salicylic acid solution through the reactor at 120 cm^3 min^{-1}. In the presence of a 25 mg TiO$_2$ layer, an obvious decrease in concentration occurred with illumination time. Further increases in the thickness of the TiO$_2$ layer; 50 mg, 75 mg, 100 mg and 125 mg, resulted in an increase in the decomposition rate but at a diminishing rate. Finally, it was reported that photooxidation of salicylic acid on TiO$_2$ films followed first–order kinetics.

Weng et al. (1997) investigated the effects of parameters, such as surface loading, pH, temperature and ionic strength, on the adsorption of chromium (VI) onto TiO$_2$ particles. pH was the key factor affecting the adsorption characteristics. The chromate adsorption was favorable under acidic conditions and the adsorbed quantity decreased with increasing pH and surface loading. Decreasing temperature and ionic strength caused increasing the adsorption capacity. Up to 90% of chromium (VI) removal was achieved with 1 g/L of TiO$_2$ in a solution containing 10^{-5} M chromium (VI).

Hilmi et al. (1999) used a glass plate coated with TiO$_2$ in a photocatalytic process to collect mercury, lead, copper and cadmium from an aqueous solution containing individual metals and mixtures. TiO$_2$ was deposited on the glass plate from a suspension of TiO$_2$ (1.4 g/L). The TiO$_2$ suspension (1 mL) was spread on one side of the glass and dried for 15 min on a hot plate at 100°C. The coated glass pieces were cured for 2 h in an oven at 400°C. The results of metals removal demonstrated that 100 mL solution containing 10 ppm of each metal could be treated with a 10 cm^2 TiO$_2$-coated plate to leave an undetectable amount of metal in one hour. Goeringer et al. (2001) found the synergism of photoreduction between two metal ions [Cu (II) and Cr (VI)] under UV irradiation of 2 g/L TiO$_2$. In the absence of Cu (II), 800μM Cr (VI) was not completely converted to Cr (III), even after 4 h irradiation. While the presence of 800μM Cu (II) resulted in complete Cr (VI) reduction within 20 min. In the same way, the half-life for the photoreduction of 600 μM Cu(II) decreased from 1 h with no Cr(VI) to 5 min in the presence of 1.6 mM Cr (VI).

Schrank et al. (2002) studied photocatalytic reactions using chromium (VI) and dye in single and mixed systems. In the single system, both chromium (VI) and dye were degraded in acidic pH. In neutral pH, chromium (VI) was not reduced, while

dye was almost completely oxidized by both acidic and neutral conditions. In the mixed system, the reduction of chromium (VI) was faster than in the single system as dye was oxidized by photo-excited holes that prevented electron-hole recombination and promoted photoreduction of chromium (VI) on TiO_2. On the other hand, the oxidation of dye was also faster in the mixed system than in the single system as a result of the prevention of electron-hole recombination by chromium (VI).

Watcharenwong (2003) investigate the removal of chromium (VI) from the synthesis wastewaters by suspended TiO_2. The parameters that emphasize are pH, the concentration of chromium (VI) solution, the amount of suspended TiO_2 and the effect of another ion, which decrease photocatalytic activity. The results shown that, the optimum pH is 3 which 59.4% efficiency, increase the concentration of chromium (VI) can decrease K_{obs} value, the reaction rate of this research is pseudo-first-order, adding of formate ion can increase the efficiency with 82.46% But in the other hand, another ions such as chloride, phosphate, sulphate, etc can decrease photocatalytic activity.

Kanki et al. (2004) investigated the photocatalytic reduction of cupric ion by TiO_2. The TiO_2 particles were suspended in the aqueous solution of copper sulphate where sodium formate was added as a hole scavenger. It was shown that cupric ion can be reduced and deposited on TiO_2 surface very rapidly when the TiO_2 particles are embedded at adequately higher densities (200 mg/l in this experiment) and formic acid is added at moderate concentrations comparative to or higher than that of cupric ion. The deposition rate depends strongly on the concentration of sodium formate: it increases as the concentration increases. The mechanism of photoreduction reaction was estimated by the elementary reactions and the adsorption of formic anion. The practical deposition rates can be successfully explained by assuming that the kinetic step of elementary oxidation reaction of adsorbed formic anion by OH radical is rate controlling, with the remaining steps being all instantaneously fast.

Sobczyński et al. (2004) studied the mechanism of phenol photocatalytic decomposition and its intermediates in the presence of illuminated TiO_2. While illuminating TiO_2, they found that the major intermediates were hydroquinone, p-benzoquinone and catechol. After completion of the reaction, only four compounds;

carbon dioxide, water, formic acid and acetic acid, were identified. In addition, the reaction of phenol decomposition showed a first-order behavior.

Habibi et al. (2005) studied effect of operational parameters on the photocatalytic degradation of three textile azo dyes in aqueous TiO_2 suspensions under high-pressure mercury lamp irradiation (400 W). Results indicate that the photocatalytic degradation of three dyes in water on TiO_2 photocatalyst is very different. The photocatalytic degradation increased with increasing initial concentration of dye, amount of photocatalyst, and UV-irradiation time, by contrast decreased with increasing inorganic ions concentration. While the addition of oxygen flux and solution temperature reduces time of degradation. Optimal UV-irradiation wavelength and solution pH is very different. The difference was due to the difference in physicochemical properties of three diazo dyes. In addition, the presence of inorganic ions such as SO_4^{2-}, Cl^- and NO_3^- that are frequently found to co-exist with azo dyes in industrial effluent generally decreased the photocatalytic degradation rate of the whole dyes. The complete mineralization was confirmed using the chemical oxygen demand measurements and formation of inorganic ions such as NH_4^+, NO_3^-, NO_2^-, Cl^- and SO_4^{2-}.

Mohapatra et al. (2005) studied the photocatalytic reduction of chromium (VI) in aqueous solution over sulphate modified TiO_2. Samples of different crystal forms and sizes of unmodified and sulphate modified TiO_2 were prepared by varying pH, source and concentration of sulphate ion and by activating at different temperatures. Samples prepared at lower pH show more surface area than that of higher pH and sulphate modified TiO_2 can be effectively used for reduction of chromium (VI) under solar radiation. The percentage of photocatalytic reduction of chromium (VI) under solar radiation is higher at low pH and decreases with rise in pH of suspension. Presence of sacrificial electron donor (in this research is EDTA) enhances the photocatalytic reduction whereas presence of oxygen reduces it. The photocatalytic reduction of chromium (VI) depends on surface area, the crystal form and particle size of TiO_2. Samples containing mixtures of anatase and rutile phases exhibit highest activity for reduction of chromium (VI) than that of single phases.

2.2 Fixed bed photocatalytic reactor (FBPR)

A number of photocatalytic reactors have been patented in recent years but none has so far been developed to pilot-scale level. Based on the manner in which the catalyst is used, and on the arrangement of the light source and the reactor vessel, all photoreactor configurations fall under 4 categories. They are slurry-type in which the catalyst particles are in suspension form, immersion-type with lamps immersed within the reactor, external-type with lamps outside the reactor, and distributive-type with the light distributed from the source to the reactor by optical means, such as reflectors and light conductors or optical fibers. Fixed bed photoreactor group in external-type in which the catalyst is immobilized on the reactor wall, on a mess of fiberglass, on glass and stainless steel, etc with lamp outside the reactor.

In this reactor, wastewaters was fed into a reactor and pass through a media that is coated catalyst while mixing of the wastewaters is achieved by turbulent flow of wastewaters stream. When irradiation of UV lamp goes through reactor, the photocatalysis process occurs. The contaminants were reacted with catalyst and attach to surface of the media. The fixed-bed reactor had originally been developed for the solar application of the photocatalytic purification of polluted water.

2.2.1 Advantage of fixed bed photocatalytic reactor

Advantages of fixed bed photocatalytic reactor are as follow:

- this photoreactor provides a well light distribution in which the immobilize TiO_2 receives ultraviolet light directly from the source

- with photoreactor configuration, this type of reactor can be used for both artificial and solar light

- this type of reactor can make a high benefit from a fixed bedplate. By receiving the ultraviolet light throughtout the plate, mass transfer limitation is less significant during the degradation period

2.2.2 Application of fixed bed photocatalytic reactor (FBPR):

Nogueira and Jardim (1996) studied in photodestruction of dichloroacetic acid (DCA) using the solar TiO_2 thin film fixed bed reactor immobilized on a glass plate. It found lesser slopes of the plate more effective because the thickness of fluid film is higher as it flows by gravity effect on a longer retention time. The result shown that the increase of solar light intensity (365 nm, 20 to 30 W/m^2) is increase photo-degradation rate of DCA. Reactor performance with different feed flow rates suggested that no mass transfer limitations occurred since a thin fluid film was formed over the catalyst surface, make increase of flow rate increased photo-degradation rate. An exponential decay of degradation with the increase of molar flow rate was observed. As a consequence, higher degradation was observed for lower molar flow rates.

Bekbnet et al., (1996) investigated two different photocatalysts, namely Hombikat UV100 (Sachtleben Chemic) and P25 (Degussa) for comparison of their ability to degrade the toxic components of a biologically pretreated landfill leachate. In batch reactor under artificial solar UV-irradiation, the result shown a strong adsorption of the pollutant molecules was observed for both TiO_2-powders, with a maximum of almost 70% TOC reduction for Hombikat UV100, making it almost impossible to compare the degradation rate with the two catalysts in the batch system. The photocatalytic activity of Hombikat UVI00 was again tested using a thin-film fixed-bed reactor (TFFBR) configuration under UV-irradiation and continuous recirculating conditions. Here the catalyst was fixed onto a glass-plate. The highest degradation rate was observed between pH 3 and pH 7 with a maximum at pH 5, while at pH 9 and 11 the degradation was rather slow. Photonic efficiencies (ζ) based on the amount of incident irradiation have been calculated for the experiments, ζ could be increased by a reduction of the light intensity. No beneficial effect was obtained by the addition of H_2O_2 or $Na_2S_2O_8$. The addition of H_2O_2 had an inhibiting effect (at pH 7), while in the presence of $Na_2S_2O_8$ a dark degradation was observed.

Feitz et al., (2000) studied two large pilot scale fixed-bed reactor, namely coated-mesh reactor (CMR) and packed-bed reactor (PBR) that evaluated by assessing the processing rate for 2 mgl^{-1} phenol solutions. Taking into account total

volume treated and reactor surface area, processing rates for the packed-bed and coated-mesh reactors were 140 mg m^{-2} h^{-1} and 20 mg m^{-2} h^{-1}, respectively. The significantly lower degree of removal for the coated-mesh reactor is attributed to insufficient surface contact times, low levels of available attached TiO$_2$ and a small reactor to tank volume ratio. The PBR achieved rapid 99.3% removal of low levels of phenol under mostly sunny conditions. Degradation was light dependent suggesting that the dominant removal mechanism is photocatalytic degradation, not air stripping or adsorption. Lowering the pH to 3 did not enhance removal under the conditions of this study. Photonic efficiencies for 100 mg l^{-1} dichloroacetic acid mineralization in the packed bed reactor are only 40% lower than ideal suspension efficiencies.

Dijkstra et al., (2001) compared the photocatalytic degradation of formic acid of different three reactor types, namely suspended type, tubular type with coated on reactor wall and packed bed type with coated glass beads. In the suspended and the packed bed reactor appeared low pseudo-zero-order kinetics and both these systems had no mass transfer limitations. On the other hand, the tubular reactor with the catalyst coated on the wall did suffer from mass transfer limitation. The performance of the packed bed reactor with high amounts of catalyst present in the reactor was better for the larger glass beads.

Mehrvar et al., (2002) investigated the preliminary analysis of a tellerette packed-bed photocatalytic reactor in which TiO$_2$ was immobilized on stainless steel tellerette packings. The experiments revealed that mass transfer limitations in this packed bed photoreactor were not significant. However, the need with respect to optimizing the tellerette dimensions, bed radius and photocatalytic performance could be investigated. It may have more potential.

Tuprakay and Liengcharemsit (2005) studied the lifetime and regeneration of immobilized TiO$_2$ for removal of Cr (VI) in aqueous solution using TiO$_2$ fixed bed batch reactor, TiO$_2$ immobilized on polyester resin. High reduction capacity was obtained at 25 ppm initial chromium (VI) concentration under 171 W/m^2 light intensity. Adsorption capacity increased with increasing initial chromium (VI) concentration, and the area of immobilized TiO$_2$ limited the reduction efficiency. The lifetime of fresh TiO$_2$ was approximately 14 h for adsorption and it was unnecessary

to regenerate TiO_2 for the reduction reaction. In addition, it was found that the NaOH of 3.00 M concentration is a suitable solution for regenerating TiO_2 immobilized on polyester resin. Result show that the fresh TiO_2 was more active in reduction of chromium (VI) to chromium (III) than regenerated TiO_2, while the regenerated TiO_2 could adsorb chromium more than fresh TiO_2.

2.3 Chromium

2.3.1 Properties and roles of chromium

Chromium is a blue-white metal that is hard, brittle and very corrosion resistant. Chromium can be polished to form a very shiny surface and is often plated to other metals to form a protective and attractive covering. Chromium is added to steel to harden it and to form stainless steel, a steel alloy that contains at least 10% chromium. Other chromium-steel alloys are used to make armor plate, safes, ball bearings and cutting tools.

Table 2.1 The properties of chromium

(http://www.lenntech.com/Periodic-chart-elements/Cr-en.htm)

Atomic number	24
Atomic mass	$51.996 \ g.mol^{-1}$
Electronegativity	1.6
Density	$7.19 \ g.cm^{-3}$ at 20°C
Melting point	1875 °C
Boiling point	2672 °C
Vanderwaals radius	0.127 nm
Ionic radius	0.061 nm (+3) ; 0.044 nm (+6)
Isotopes	6
Electronic shell	[Ar] $3d^5 \ 4s^1$
Energy of first ionisation	651.1 kJ.mol -1
Standard potential	- 0.71 V (Cr^{3+} / Cr)
Oxidation states	+6,+3,+2

2.3.2 Chemistry of chromium

Chromium is present in the environment in several different forms. The most common forms are chromium (0), chromium (III), and chromium (VI). No taste or odor is associated with chromium compounds. Chromium (III) occurs naturally in the environment and is an essential nutrient. Chromium (VI) and chromium (0) are generally produced by industrial processes. The metal chromium, which is the chromium (0) form, is used for making steel. Chromium (VI) and chromium (III) are used for chrome plating, dyes and pigments, leather tanning, and wood preserving. Chromium (III) is comparatively insoluble while Chromium (VI) is quite soluble and is readily leached from soil to groundwater or surface water.

Chromium (III) was found in complex compound such as Cr^{+3}, $Cr(OH)^{+2}$, $Cr(OH)_3^0$ and $Cr(OH)_4^-$ that show in Figure 2.4. Chromium (III) can be removed by precipitation. It is insoluble when pH increases. Suitable pH for removal of chromium (III) is approximately 8.5 that chromium (III) is precipitated in sediment of chromium hydroxide ($Cr(OH)_3$). Figure 2.5 shows solubility of chromium hydroxide in each pH.
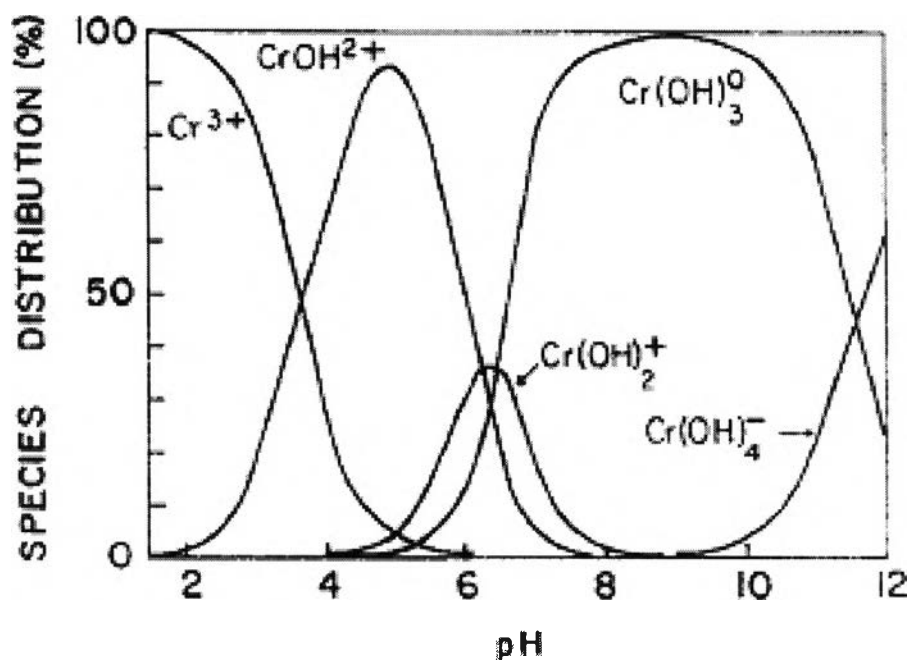

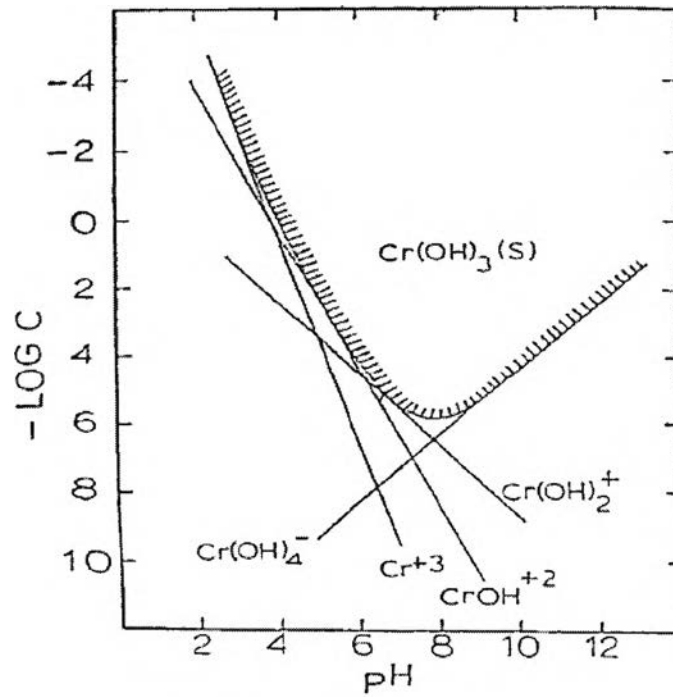Figure 2.4 Species of chromium (III) at different pH (Rai et al., 1987)

Figure 2.5 Solubility of chromium hydroxide (Kim, 1976)

Usually, chromium (VI) is quite stable and soluble in every pH. The form of chromium (VI) in the solution is CrO_4^{2-}, $HCrO_4^-$ or H_2CrO_4. These forms depend on pH value and the concentration of chromium solution. Figure 2.6 shows species of chromium (VI) at different pH.
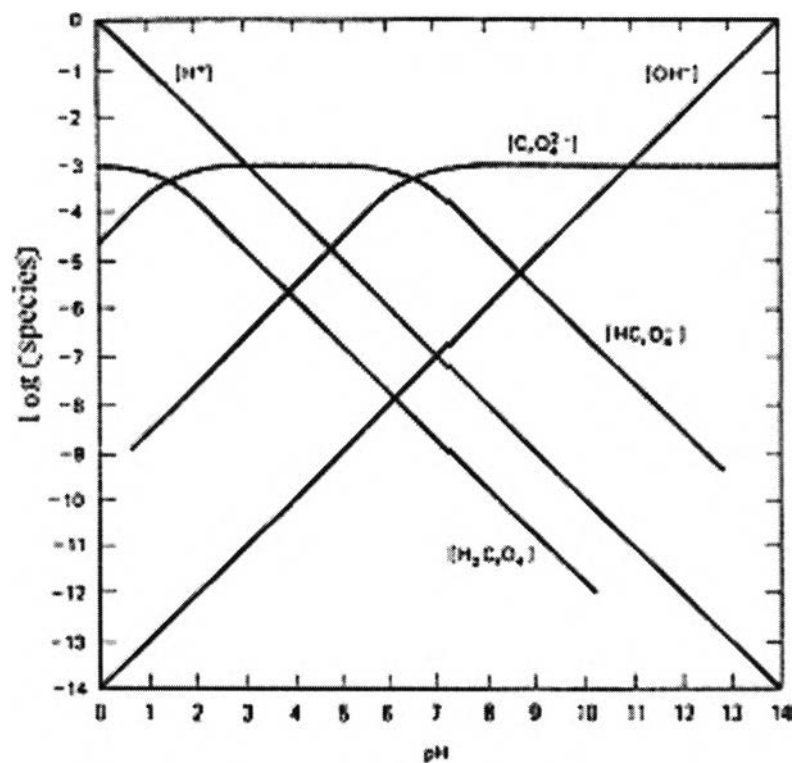

Figure 2.6 Conversion of chromium (VI) at different pH (Ku et al., 2001)

Lin et al. (1993) study the changing in the potential value of valence band (VB) and conduction band (CB) of TiO_2 was changed following the pH of the solution. It could be explained that when increasing pH of the solution, it was reduce the potential value of the band gab of TiO_2 as call *Nerstain* as change -59 mv in every changing pH at 25 °C (-59 mv/ pH Unit at 25 °C). Figure 2.7 shows reduction potential values of TiO_2 and chromium (VI) at pH 3, 7 and 11.
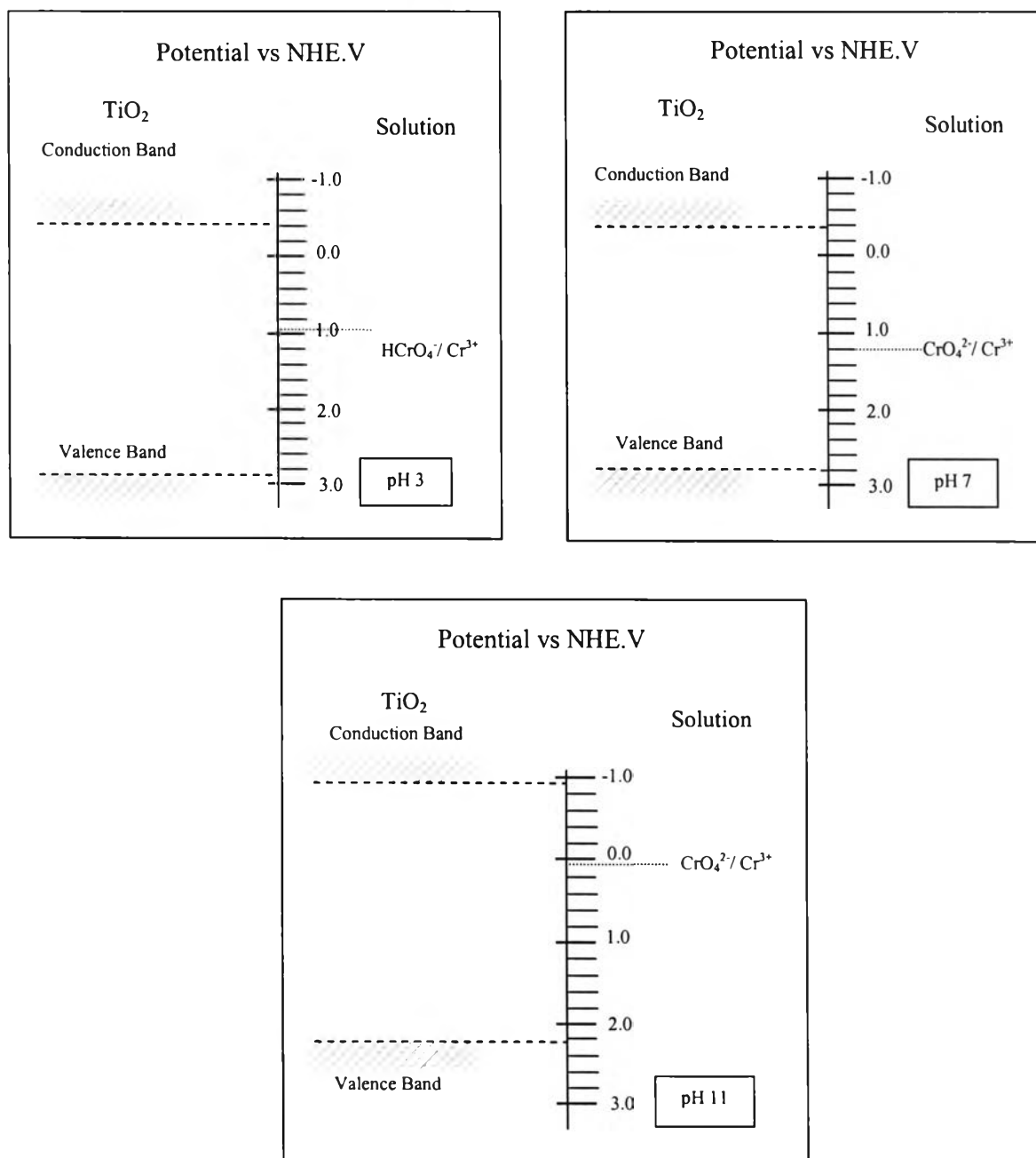

Figure 2.7 Reduction potential values of TiO_2 and chromium (VI) at pH 3, 7 and 11 (Adapted from Chenthamarakshan et.al., 2000)

2.3.3 The toxicity and contamination of chromium

The health hazards associated with exposure to chromium are dependent on its oxidation state. The metal form (chromium as it exists in this product) is of low toxicity. The trivalent form is shortages may cause heart conditions, disruptions of metabolisms and diabetes. But the uptake of too much chromium (III) can cause health effects as well, for instance skin rashes. The hexavalent form is toxic. Adverse effects of the hexavalent form on the skin may include ulcerations, dermatitis, and allergic skin reactions. Inhalation of hexavalent chromium compounds can result in ulceration and perforation of the mucous membranes of the nasal septum, irritation of the pharynx and larynx, asthmatic bronchitis, bronchospasms and edema. Respiratory symptoms may include coughing and wheezing, shortness of breath, and nasal itch.

There are several different kinds of chromium that differ in their effects upon organisms. Chromium enters the air, water and soil in the trivalent and hexavalent form through natural processes and human activities.

The main human activities that increase the concentrations of chromium (III) are steal, leather and textile manufacturing. The main human activities that increase concentrations of chromium (VI) are chemical, leather and textile manufacturing, electroplating and other chromium (VI) applications in the industry. These applications will mainly increase chromium concentrations in water. Through coal combustion chromium will also end up in air and through waste disposal chromium will end up in soils.

Most of the chromium in air will eventually settle and end up in waters or soils. Chromium in soils strongly attaches to soil particles and as a result it will not move towards groundwater. In water chromium will absorb on sediment and become immobile. Only a small part of the chromium that ends up in water will eventually dissolve.

Crops contain systems that arrange the chromium-uptake to be low enough not to cause any harm. But when the amount of chromium in the soil rises, this can still lead to higher concentrations in crops. Acidification of soil can also influence chromium uptake by crops. Plants usually absorb only chromium (III). This may be

the essential kind of chromium, but when concentrations exceed a certain value, negative effects can still occur.

Chromium is not known to accumulate in the bodies of fish, but high concentrations of chromium, due to the disposal of metal products in surface waters, can damage the gills of fish that swim near the point of disposal.

In animals chromium can cause respiratory problems, a lower ability to fight disease, birth defects, infertility and tumor formation.

2.4 Sol-Gel Process

The sol-gel process is a versatile solution process for making ceramic and glass materials. In general, the sol-gel process involves the transition of a system from a liquid "sol" (mostly colloidal) phase into a solid "gel" phase. Applying the sol-gel process, it is possible to fabricate ceramic or glass materials in a wide variety of forms: ultra-fine or spherical shaped powders, thin film coatings (Vossen and Kern, 1991), ceramic fibers, microporous inorganic membranes, monolithic ceramics and glasses, or extremely porous aerogel materials. An overview of the sol-gel process is presented in a simple graphic work below.

The starting materials used in the preparation of the "sol" are usually inorganic metal salts or metal organic compounds such as metal alkoxides. In a typical sol-gel process, the precursor is subjected to a series of hydrolysis and polymeration reactions to form a colloidal suspension, or a "sol" (Klein, 1988). Further processing of the "sol" enables one to make ceramic materials in different forms. Thin films can be produced on a piece of substrate by spin-coating or dip-coating. When the "sol" is cast into a mold, a wet "gel" will form. With further drying and heat-treatment, the "gel" is converted into dense ceramic or glass articles. If the liquid in a wet "gel" is removed under a supercritical condition, a highly porous and extremely low density material called "aerogel" is obtained (Brinker and Scherer, 1990). As the viscosity of a "sol" is adjusted into a proper viscosity range, ceramic fibers can be drawn from the

"sol". Ultra-fine and uniform ceramic powders are formed by precipitation, spray pyrolysis, or emulsion techniques.

2.5 Photocatalytic kinetic reactions

The kinetic reactions that occur in photocatalytic process:

2.5.1 Zero order reactions

Zero order reactions are reaction whose rates are independent of reactant concentrations. These reactions occur at low concentration of pollutant which amount of catalyst exceed amount of pollutant. The kinetic coefficient (k) can be determined by following equation:

$$-\frac{d[C]}{dt} = k[C]^n \tag{5}$$

$$-\frac{d[C]}{dt} = k[C]^0 \tag{6}$$

$$C = C_0 - kt \tag{7}$$

Where k is the kinetic coefficient or reaction rate (mg/L.min)

n is the order of the reaction

C is the concentration at time (mg/L)

C_0 is the concentration at beginning (mg/L)

From zero order equation, it can be determined kinetic coefficient from the slope of graph between concentrations with reaction time.

2.5.2 Pseudo-first order reactions

Pseudo-first order reactions are reaction whose rates are dependent on the concentration of only one reactant. These reactions occur at high concentration of pollutant which amount of pollutant exceed amount of catalyst. The kinetic coefficient (k) can be determined by following equation:

$$-\frac{d[C]}{dt} = k_{obs}[C]^n \tag{8}$$

$$-\frac{d[C]}{dt} = k_{obs}[C]^1 \tag{9}$$

$$-\ln\left[\frac{C}{C_0}\right] = k_{obs}t \tag{10}$$

Where k_{obs} is the pseudo-first order kinetic rate constants, (min^{-1})

n is the order of the reaction

C is the concentration at time, (mg/L)

C_0 is the concentration at beginning, (mg/L)

From pseudo-first order equation, it can be obtained the k_{obs} values for each initial concentration from the slope of graph between $-\ln\left[\frac{C}{C_0}\right]$ with reaction time which these k_{obs} values use to determined the adsorption equilibrium constants and kinetic coefficient by Langmuir-Hinshelwood equation.

2.5.3 Langmuir-Hinshelwood reaction kinetics

Langmuir-Hinshelwood kinetics (L-H) model is commomly used for quantitative description of heterogeneous phase reactions between two adsorbed reactants that take place on the interface of two systems. It has also been efficient as a standard quantitative description of liquid-solid reactions (Al-Ekabi et al., 1988). Extrapolation of L-H model for liquid-solid reactions requires some modification for TiO_2 solid surface in aqueous suspension, since hydroxyl groups and water molecules cover it.

The competitive analysis of the kinetic in the photocatalytic reduction of contaminants via irradiated semiconductors, TiO_2 distinguishes five situations as follow:

1) The reaction take place between two adsorbed reagents;

2) The reaction occur between a redical in the solution and the adsorbed reagent;

3) The reaction take place between the radical linked to the surface and the reagents in the solution;

4) The reaction occurs with both species in the solution;

5) The adsorption process occurs on mono layer.

Therefore, for the standard L-H information, it is assumed that the reaction occurs on the surface of the substrate. In photocatalytic (or photoadsorption) reactions, the rate dependence on reagent concentration that can be approximated by the equation:

$$r = -\frac{dC}{dt} = \frac{kKC}{(1+KC)}, r = k_{obs}.C \qquad (11)$$

$$\frac{1}{r} = \frac{1}{kKC} + \frac{KC}{kKC} \qquad (12)$$

$$\frac{1}{r} = \frac{1}{kKC} + \frac{1}{k} \qquad (13)$$

$$\frac{C}{r} = \frac{C}{kKC} + \frac{C}{k} \qquad (14)$$

$$\frac{1}{k_{obs}} = \frac{1}{kK} + \frac{C}{k} \qquad (15)$$

Where r is the initial rate of disappearance of the contaminants, mg/L.min.

k is an apparent reaction rate constants which is related to the adsorption/desorption affinity. It depends on light intensity, mg/L.min.

K is the Langmuir constant reflecting the adsorption equilibrium between the reagent and the surface of the photocatalyst, L/mg.

C is the reactant concentration, mg/L.

k_{obs} is the reaction rate constant, min^{-1}.

From this equation, it can be determined the adsorption equilibrium constants and kinetic coefficient by plotting graph between $\frac{1}{k_{obs}}$ with reaction time. The slope of this graph equal to $\frac{1}{k}$ and y-axis intersection equal to $\frac{1}{kK}$.

2.6 Debye-Scherrer equation

It can be determined the crystallite size of catalyst by Debye-Scherrer equation as follow:

$$L = \frac{K\lambda}{\beta \cos \theta}$$
(16)

Where L represents the crystallite size, (nm)

K as the Debye-Scherrer constant, (Usually taken as 0.89)

λ as the wavelength of the X-ray radiation, (CuKα = 0.15418 nm)

β as the line width of half-maximum height of the broadened peak

θ as the half diffraction angle of the controid of the peak, (degree)